Available online at www.sciencedirect.com
ScienceDirect
Magnetic Resonance Imaging 24 (2006) 1295–1302
MAGNETIC RESONANCE IMAGING

Considerations in applying 3D PRESS H-1 brain MRSI with an eight-channel phased-array coil at 3 T

Yan Li[a,b], Joseph A. Osorio[a,b], Esin Ozturk-Isik[a,b], Albert P. Chen[a,b], Duan Xu[a,b], Jason C. Crane[b], Soonmee Cha[b,c], Susan Chang[c], Mitchel S. Berger[c], Daniel B. Vigneron[a,b], Sarah J. Nelson[a,b,d,*]

[a]*UCSF/UCB Joint Graduate Group in Bioengineering, San Francisco, CA 94720, USA*
[b]*Department of Radiology, University of California, San Francisco, CA 94143, USA*
[c]*Department of Neurological Surgery, University of California, San Francisco, CA 94143, USA*
[d]*Program in Bioengineering, University of California, San Francisco, CA 94158-2330, USA*

Received 23 December 2005; accepted 20 July 2006

Abstract

The purpose of this study was to assess the benefits of a 3 T scanner and an eight-channel phased-array head coil for acquiring three-dimensional PRESS (Point REsolved Spectral Selection) proton (H-1) magnetic resonance spectroscopic imaging (MRSI) data from the brains of volunteers and patients with brain tumors relative to previous studies that used a 1.5 T scanner and a quadrature head coil. Issues that were of concern included differences in chemical shift artifacts, line broadening due to increased susceptibility at higher field strengths, changes in relaxation times and the increased complexity of the postprocessing software due to the need for combining signals from the multichannel data. Simulated and phantom spectra showed that very selective suppression pulses with a thickness of 40 mm and an overpress factor of at least 1.2 are needed to reduce chemical shift artifact and lipid contamination at higher field strengths. Spectral data from a phantom and those from six volunteers demonstrated that the signal-to-noise ratio (SNR) in the eight-channel coil was more than 50% higher than that in the quadrature head coil. For healthy volunteers and eight patients with brain tumors, the SNR at 3 T with the eight-channel coil was on average 1.5 times higher relative to the eight-channel coil at 1.5 T in voxels from normal-appearing brains. In combination with the effect of a higher field strength, the use of the eight-channel coil was able to provide an increase in the SNR of more than 2.33 times the corresponding acquisition at 1.5 T with a quadrature head coil. This is expected to be critical for clinical applications of MRSI in patients with brain tumors because it can be used to either decrease acquisition time or improve spatial resolution.

Keywords: Proton magnetic resonance spectroscopic imaging; Eight-channel phased-array coil; 3 T; Very selective suppression; Brain tumors

1. Introduction

Previous studies have shown that three-dimensional (3D) proton (H-1) magnetic resonance spectroscopic imaging (MRSI) is important for the evaluation of the spatial extent and metabolic characterization of primary brain tumors [1–6]. There are a number of resonances from the different compounds in the brain that can be detected in proton spectra. Choline-containing compounds (Cho), creatine (Cr), *N*-acetyl aspartate (NAA), lactate (Lac) and lipid (Lip), which are observed in spectra acquired with long echo times (TE=144 ms), are important metabolic markers. General markers of brain tumors are the elevation of Cho, which is due to increased membrane synthesis in neoplasms, and the reduction of the neuronal marker NAA. The Cho/NAA index allows for a comparison between subjects and has been used to identify metabolic abnormality in brain tumors [7]. Furthermore, Cr reflects cellular bioenergetics, Lac is a

Presented in part at the 13th Annual Meeting of the ISMRM—2005, Miami, FL, USA

* Corresponding author. Department of Radiology, University of California, San Francisco, Box 2532, Byers Hall, 1700 4th St., San Francisco, CA 94143-2532, USA. Tel.: +1 415 476 6383; fax: +1 415 514 2550.
E-mail address: nelson@mrsc.ucsf.edu (S.J. Nelson).

0730-725X/$ – see front matter © 2006 Elsevier Inc. All rights reserved.
doi:10.1016/j.mri.2006.07.012

marker of anaerobic metabolisms and Lip, likely a marker of necrosis, is highly associated with high-grade tumors. These markers together have been used in the investigation of diagnosis, grading, therapy and prognosis for patients with brain tumors.

PRESS (Point REsolved Spectral Selection) is one of the localization techniques available for obtaining multi-voxel H-1 MRSI. It is well known that the PRESS volume selection results in spatial variations in metabolite ratios on the edge of the selected volume due to chemical shift artifacts. These errors are dependent on the bandwidth of PRESS pulses, the size of the selected region and the resonant frequency and will therefore become more prominent as the field strength increases. One way to reduce the effect of the chemical shift artifact is to prescribe a PRESS box larger than the region of interest (overpress) and to use very selective suppression (VSS) pulses [8], which have much sharper spatial transition bands as compared with traditional outer volume suppression (OVS), to suppress signals arising from beyond the region of interest. Although VSS pulses and overpress have been applied at 1.5 T to reduce chemical shift artifacts in one study [8], it was not clear whether corresponding pulses designed for use at 3 T could cope with the increased magnitude of the effect.

Previous studies using single-voxel and spectroscopic imaging of the human brain have been applied at 3 T [9–12] and have inferred an increase in the signal-to-noise ratio (SNR) and spectral resolution relative to studies that have been applied at 1.5 T [13–15]; however, the magnitude of the increase was variable. Concerns as to the effect of changes in longitudinal and transverse relaxation times of metabolites [16,17] and whether increased susceptibility effects in patients with brain tumors would compromise data quality have also been expressed. While the use of phased arrays for MR spectroscopy has been demonstrated [18–21], methods for combining the data from multichannel radiofrequency coils have not yet been fully explored in a clinical setting.

The purposes of this study were to determine which parameters are important for obtaining reliable spectra from patients with brain tumors at 3 T and to compare the data obtained with similar findings at 1.5 T. The issues that were considered included the chemical shift artifacts for different VSS and overpress factors, the variations in linewidth at 1.5 versus 3 T, the differences in SNRs between the quadrature head coil and the eight-channel phased-array coil and how the details of the data acquisition and postprocessing influence the quality of the spectra. These parameters were explored through simulations and measurements from phantoms, healthy volunteers and patients with brain tumors.

2. Methods

2.1. Simulated data

Spectral data were simulated to assess the effects of VSS pulses and overpress factors as described previously [22]. The overpress factor is defined as the ratio of the linear dimension of the excited volume to the prescribed volume. The objects of simulation were a uniform phantom and an elliptical normal brain. The spectra were created using Lorentzian peak shapes with linewidths of 2 Hz, 512 dwell points and a sweepwidth of 1000 Hz for 1.5 T spectra and Lorentzian peak shapes with linewidths of 4 Hz, 1024 dwell points and a sweepwidth of 2000 Hz for 3 T spectra. Water suppression was set at 20:1. The Cho/Cr/NAA/Lac relative ratio was 0.5:0.5:1:0.25. The PRESS volume selection pulses were simulated with bandwidths based on the default values used in the product pulse sequences on the 3 T MR scanner. These were 933 Hz for the 180° pulse and 2400 Hz for the 90° pulse. The pulse profiles were simulated to be either ideal (rectangular) or based on empirical profiles of the selected volume acquired on a uniform phantom. The sizes of the selected volumes were the same for all simulated data. VSS pulses were simulated as having a rectangular profile of either 30 or 40 mm in thickness, and the efficacy of suppression was assumed to be 90%. The overpress factors considered were 1.0, 1.1, 1.2 and 1.3, with a phase-encoding matrix of 16×16×8.

2.2. MR data

Empirical data were obtained from a head phantom, from 6 volunteers and from 12 patients using either a standard transmit/receiver quadrature head coil or an eight-channel receive-only phased-array coil on 1.5 T and 3 T GE EXCITE scanners (GE Healthcare Technologies, Waukesha, WI, USA). The MR scans included the acquisition of anatomical and spectroscopic imaging data.

2.2.1. MRI

Anatomical MR images were composed of T_1-weighted *sagittal scout images* (TR/TE=54/2 ms at 1.5 T and 70/2 ms at 3 T), axial FLAIR (FLuid Attenuated Inversion Recovery; TR/TE/TI=10002/123/2200 ms at 1.5 T and 10002/127/2200 ms at 3 T) and T_1-weighted SPGR (SPoiled GRadient echo) images (TR/TE=8/2 ms at 1.5 T and 26/3 ms at 3 T).

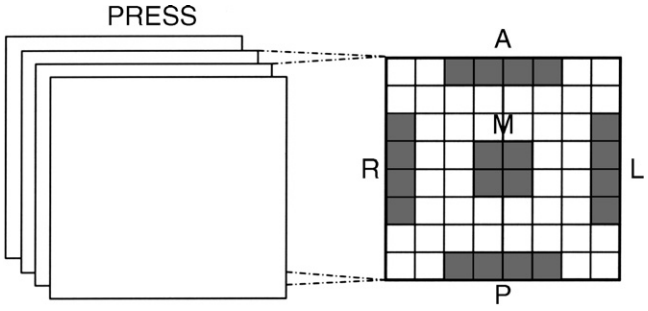

Fig. 1. H-1 PRESS MRSI applied in studies on chemical shift artifacts from a simulation and the phantom. The size of the excited volume was 80×80×40 mm^3 in all data sets. Chemical shift artifacts on the R, L, A and P sides were calculated from the average of the central two slices. The middle voxels (M), which have the least chemical shift artifacts, were used as controls.

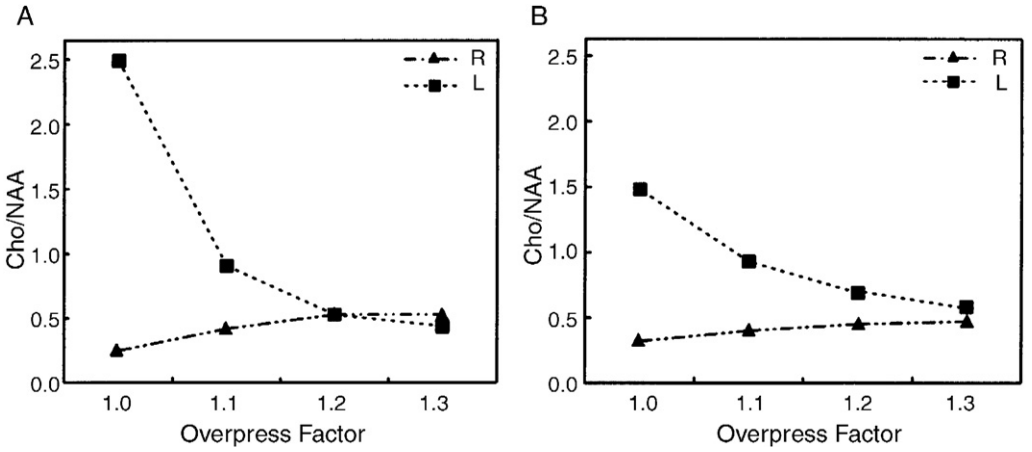

Fig. 2. Simulation of H-1 PRESS MRSI with different overpress factors. Changes in the mean Cho/NAA height value in the R–L direction of the spectra with ideal profiles (A) and empirical profiles (B) are shown. Chemical shift artifacts decrease with increases in the overpress factor. An overpress factor of 1.2 is needed to eliminate the chemical shift artifact with ideal profiles at 3 T, whereas that of 1.3 is needed with empirical profiles.

2.2.2. MRSI

The 3D H-1 MRSI data were obtained using PRESS volume selection, VSS outer volume suppression and CHESS (CHEmical Shift Selective) water suppression with TR/TE of 1100/144 ms. The PRESS volume selection used pulses with bandwidths of 933 Hz for the 180° pulse and 2400 Hz for the 90° pulse. An overpress factor of either 1.0 or 1.2 and VSS pulses of width 40 mm were prescribed around the prescribed volume. Six additional graphic VSS bands were applied adjacent to the subcutaneous lipid layer to further improve suppression. For the studies performed with the eight-channel coil, proton density-weighted GRadient Echo (GRE) images were acquired using the manufacturer-provided parallel imaging calibration sequence to obtain estimates of coil sensitivities (TR/TE=150/2 ms). The manufacturer's linear autoshim procedure was applied at 1.5 T, and its higher-order shimming procedure was performed before spectral acquisition at 3 T. The spectral data were acquired with 512 dwell points and 1000 Hz sweepwidth at 1.5 T as well as with 1024 dwell points and

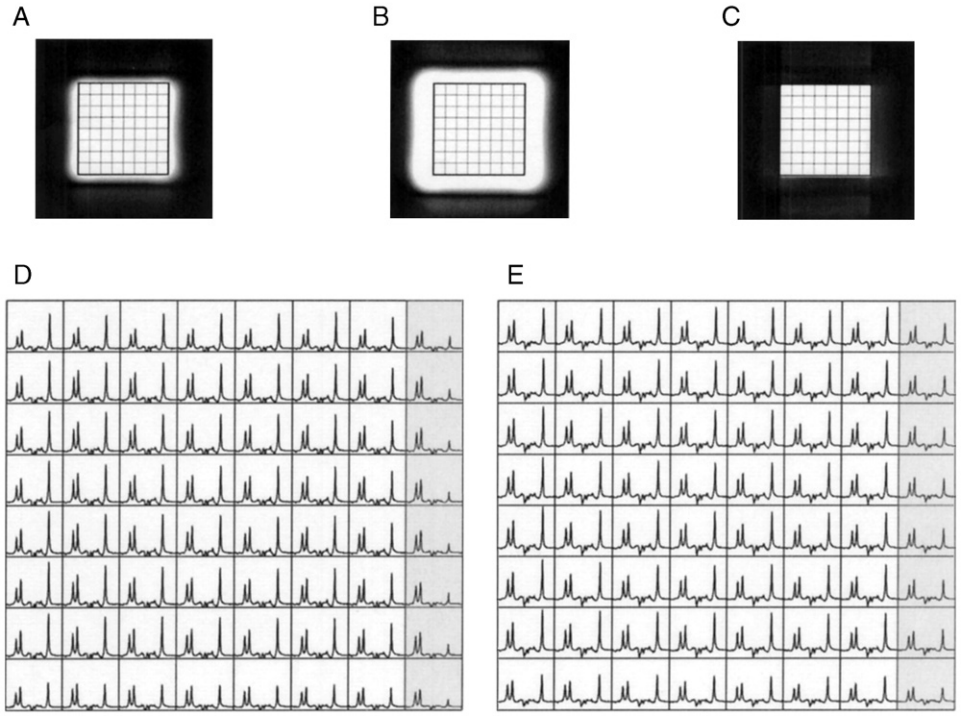

Fig. 3. The top images were scanned without VSS and with an overpress factor of 1.0 (A), with an overpress factor of 1.2 only (B), and with 40-mm VSS and an overpress factor of 1.2 (C). Panels D and E correspond to Panels A and C, respectively. The spectra from the top right corner have low Cho/NAA and Cr/NAA ratios, whereas those from the opposite corner have higher levels (D). Application of VSS and overpress significantly reduces the chemical shift artifact as seen by the differences in the relative levels of Cho and NAA in the far right column of the spectra in Panel E versus Panel D.

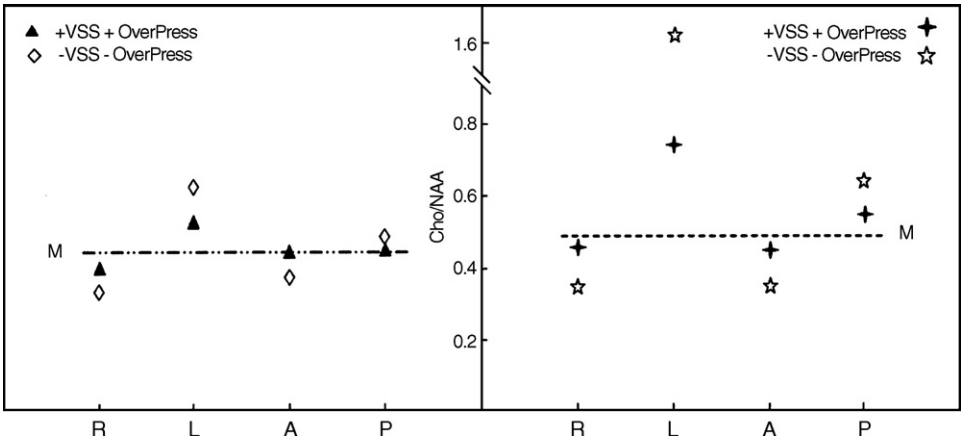

Fig. 4. Chemical shift artifact observed with an eight-channel coil at 1.5 T (left panel) and at 3 T (right panel) with/without 40-mm VSS and an overpress factor of 1.2 measured in a uniform phantom. VSS and overpress significantly reduce chemical shift artifact in the phantom data.

2000 Hz sweepwidth at 3 T. Spectral array sizes were 12×12×8 for an acquisition time of approximately 9 min and 16×16×8 for an acquisition time of approximately 17 min, acquired with *k*-space sampling restricted to an elliptical region of *k*-space and fields of view (FOVs) corresponding to a nominal spatial resolution of 1 cc [23]. The excited volumes were positioned in similar regions for each of the data sets that were going to be compared.

2.3. Study population

Phantom spectra were acquired with the standard quadrature head coil and the eight-channel phased-array head coil at both field strengths, with and without VSS and overpress factors of 1.0 and 1.2. Six healthy volunteers (three males and three females; median age=27 years) were scanned at 1.5 T and 3 T. To test the reproducibility of the data, we scanned the phantom and three of the volunteers a second time with another 3 T scanner from the same manufacturer with a similar eight-channel coil. Twelve patients with different kinds of primary brain tumors were involved in the study. Eight of the patients were scanned at 1.5 T and 3 T field strengths using the eight-channel coil. All of these spectra were acquired with a 16×16×8 spectral array. The other four patients were scanned with the eight-channel coil at 3 T initially with a 12×12×8 array and then with a 16×16×8 spectral array at a follow-up scan obtained 2 months later.

2.4. Postprocessing and analysis

The spectra were quantified using a previously published methodology [22]. Spectral arrays from the eight-channel coil were processed individually, and the signals were combined using in-house developed software that weights the data by their coil sensitivities. The theory of the combination for eight-channel data was based on a SENSE (SENSitivity Encoding) reconstruction with a reduction factor (*R*) of 1.0 as described in a previous article [24]. The spectral data were apodized by a 2 Hz and a 4 Hz Lorentzian filter at 1.5 T and 3 T, respectively, as a compromise between reducing noise and distinguishing between overlapping peaks. The peak parameters of the metabolites were computed automatically for each voxel within the excited region using in-house software.

For the empirical data, the 3D H-1 MRSI data were referenced to the 3D SPGR image by assuming that there was no movement between the image and spectra acquisition. The FLAIR image was aligned to the corresponding 3D SPGR image. Segmentation of the brain images was performed automatically on the 3D SPGR images using a program based on the Markov random field model [25]. The segmented white matter mask was then used to identify voxels that had at least 90% normal-appearing white matter (NAWM). These were the voxels used for comparative analyses in the volunteer and patient data.

For the study on chemical shift artifact effects in the simulated and phantom data, the mean value of the Cho/NAA ratio was calculated from the center and the right, left, anterior and posterior of the middle two slices (Fig. 1). The normal voxels for patient data were defined by restricting the analysis to voxels outside T_2 abnormalities at 1.5 T and 3 T. To avoid errors in the identification of normal voxels, we excluded the edges of the PRESS box and ventricles from the calculation. To eliminate errors due to susceptibility or other artifacts, we only included voxels if the estimated linewidths of all of their peaks were between 2 and 10 Hz. The SNRs of individual metabolites were

Table 1
SNRs of metabolites with an eight-channel coil and a quadrature head coil at 1.5 T and 3 T

	Eight-channel coil			Quadrature coil		
	Cho	Cr	NAA	Cho	Cr	NAA
Phantom						
1.5 T	105	153	234	78	108	162
3 T	220	297	428	136	183	254
3 T/1.5 T	2.09	1.94	1.83	1.75	1.70	1.57
Volunteers (n=6)						
1.5 T	31	26	59	21	17	38
3 T	47	41	89	27	24	53
3 T/1.5 T	1.52	1.58	1.51	1.29	1.41	1.39

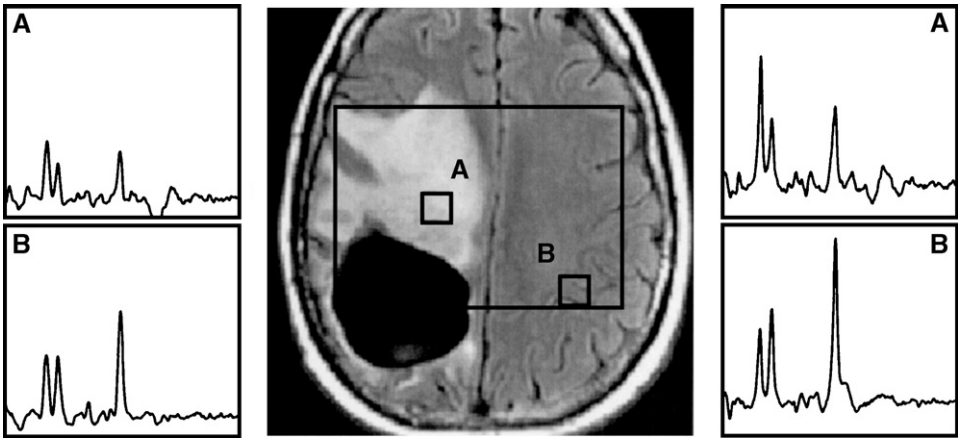

Fig. 5. MRSI for a patient with a grade IV glioblastoma multiforme at the same noise scale for acquisitions at 1.5 T (left panel) and 3 T (right panel). Voxel A comes from the tumor region, which has a higher Cho and a lower NAA, whereas voxel B is from the normal region. The vertical scales of all four spectra were adjusted to equalize the noise level of the different spectra. The spectra at 3 T have a higher SNR in the tumor and normal voxels.

estimated by dividing the heights of the peaks, Cho, Cr and NAA, by the standard deviation of the noise from the peak-free region at the right end of the spectrum [22]. Wilcoxon rank sum tests were applied to evaluate differences in SNRs, with a P value of .05 considered to be significant.

3. Results

3.1. Chemical shift artifact in the simulation

The simulations assumed that the chemical shift artifact was half as much at 1.5 T as it was at 3 T. The mean Cho/NAA height ratios for the phantom simulation with ideal profiles at 3 T were 0.25 versus 2.50, 0.42 versus 0.91, 0.53 versus 0.53 and 0.53 versus 0.44 on the right and left (R–L) edges with overpress factors of 1.0, 1.1, 1.2 and 1.3, respectively; those with the empirical profiles were 0.32/1.48, 0.40/0.93, 0.45/0.69 and 0.47/0.57 (R–L), respectively (Fig. 2). These values were compared with the true ratio of 0.5 in the simulated phantom. For simulated brain spectra at overpress factors of 1.0, 1.1, 1.2 and 1.3, respectively, the mean Cho/NAA height ratios with ideal profiles were 0.17/1.53, 0.36/0.71, 0.52/0.48 and 0.56/0.45 (R–L) as compared with 0.27/1.22, 0.37/0.82, 0.44/0.64 and 0.47/0.56 for empirical profiles. The 40 mm VSS pulses provided better lipid suppression for the simulated brain data as compared with the 30 mm VSS pulses at 1.5 and 3 T. The chemical shift artifact decreased with the overpress factor, and it was observed that an overpress factor of 1.3 was needed to entirely eliminate the chemical shift artifact for the empirical profiles at 3 T. Because of the concern that we would be exciting subcutaneous lipids for the in vivo situation, we selected an overpress factor of 1.2 and a VSS pulse of 40 mm for the phantom and in vivo human studies.

3.2. Chemical shift artifact in the phantom

Phantom data with an overpress factor of 1.0 clearly showed the chemical shift artifact on the edges of the PRESS box. The 3D MRSI with and that without VSS and with overpress factors of 1.0 and 1.2, acquired with an eight-channel coil at 3 T, are shown in Fig. 3. With VSS and an overpress factor of 1.2, the image showed a much sharper edge and the spectra had less chemical shift artifact. The chemical shift artifact with an eight-channel coil at 1.5 T and that at 3 T are illustrated in Fig. 4. At 1.5 T, the mean Cho/NAA height ratios were 0.33 versus 0.63 on the R–L edges and 0.38 versus 0.49 on the anterior and posterior (A–P) edges of the PRESS box without VSS pulses and with an overpress factor of 1.0; however, the ratios were 0.40/0.52 (R–L) and 0.44/0.45 (A–P) when VSS pulses and an overpress factor of 1.2 were used. The ratio expected from knowledge of the metabolite concentrations in the phantom was 0.5. Corresponding values at 3 T were 0.35/1.61 (R–L)

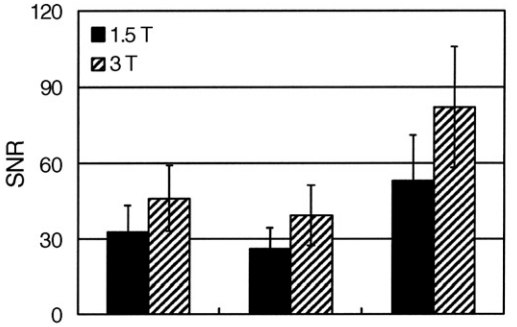

	Cho	Cr	NAA
1.5 T	32 (11)	26 (8)	53 (18)
3 T	46 (13)	39 (12)	82 (24)
3 T/1.5 T	1.44	1.50	1.55
P	<.001	<.001	<.001

Fig. 6. SNRs of metabolites with an eight-channel coil at 1.5 and 3 T from the normal voxels of eight primary brain tumor patients. Approximately 300 voxels were involved in the calculations at 1.5 and 3 T. The SNRs of Cho, Cr and NAA at 1.5 and 3 T are shown in the table (mean±S.D.). P values lower than .001 were obtained for all three metabolites for the differences in SNRs at 1.5 and 3 T by Wilcoxon rank sum tests.

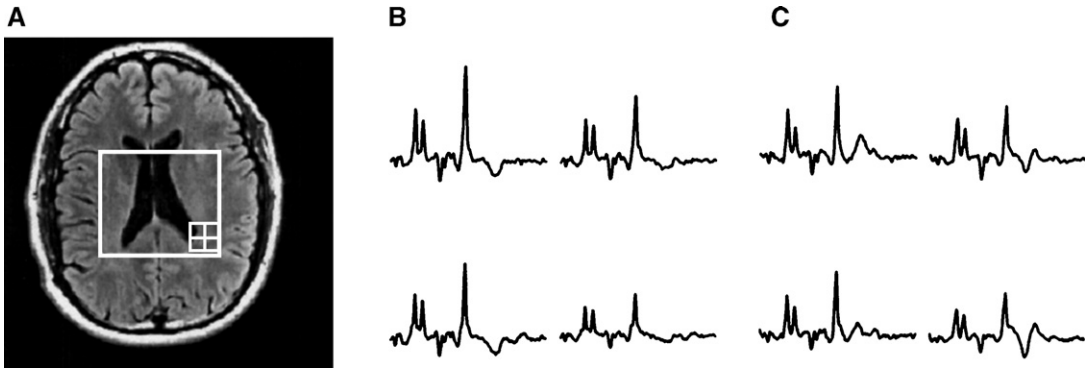

Fig. 7. (A) MRSI data from a patient with glioma with 16×16×8 (B) and 12×12×8 (C) phase-encoding arrays. The spectra with the 16×16×8 phase-encoding array (B) were positioned similarly as those with the 12×12×8 phase-encoding array (C). The vertical scales of all the spectra were adjusted to equalize the noise level of the different spectra. The spectra with the 16×16×8 phase-encoding array exhibited a higher SNR, whereas those with the 12×12×8 phase-encoding array had great lipid contamination.

and 0.35/0.65 (A–P) without VSS pulses and with an overpress factor of 1.0 as compared with 0.46/0.75 (R–L) and 0.45/0.55 (A–P) with VSS pulses and an overpress factor of 1.2. These results are consistent with the simulated data in that the chemical shift artifact at 3 T is much larger and the lower bandwidth in the R–L direction (180° pulse) caused larger errors. Applying VSS pulses with an overpress factor of 1.2 significantly reduced the artifact. Similar results were obtained from the quadrature head coil.

3.3. Coil and field strength comparison

The SNRs of spectra obtained from the phantom (with VSS pulses and an overpress factor of 1.2) and volunteers with the eight-channel coil and the quadrature head coil at 1.5 T and 3 T are given in Table 1. The SNR at 3 T with the eight-channel coil was on average 1.96 times higher in the phantom but only approximately 1.53 times higher for volunteers at 3 T relative to that at 1.5 T. The SNR in the eight-channel coil was on average 52% higher than that in the quadrature head coil at 1.5 T and was 71% higher relative to the quadrature head coil at 3 T. For the volunteer data, the SNR at 3 T with the eight-channel coil was approximately 2.33 times the SNR for data acquired at 1.5 T with the quadrature head coil. The spectra of the phantom and three volunteers that were obtained on the two 3 T scanners with eight-channel coils demonstrated similar SNR values and linewidths.

3.4. Field strength comparison for patients

Examples of MRSI acquisitions from a patient with grade IV glioma at 1.5 T and 3 T are shown in Fig. 5. Note that the spectra are scaled by the estimated standard deviation of the noise in each data set. The 3 T spectra demonstrated a higher SNR and better quality as compared with the 1.5 T data in the normal and tumor voxels. The differences in the SNR at 3 T and that at 1.5 T for the eight patients studied with the eight-channel coil with a 16×16×8 phase-encoding array were 1.44 for Cho, 1.50 for Cr and 1.55 for NAA, as shown in Fig. 6. These values are consistent with those observed in the healthy volunteers. If taken together, the SNRs of Cho, Cr and NAA from the segmented NAWM of the six volunteers and eight patients were 31±10, 24±7 and 56±17, respectively, at 1.5 T and 50±13, 41±10 and 91±24, respectively, at 3 T, which are consistent with the results shown in Table 1 and Fig. 6. When corrected for filtering, the estimated linewidths for Cho, Cr and NAA at 1.5 T were 4.5±1.2, 4.3±1.0 and 5.2±1.4 Hz, respectively, at 1.5 T and were 6.5±1.4, 6.1±1.2 and 6.9±1.3 Hz, respectively, at 3 T (values expressed as mean±S.D.). This means that, when expressed in terms of parts per million, the spectral resolution was better at 3 T relative to that at 1.5 T.

3.5. Comparison of the 12×12×8 and 16×16×8 phase-encoding arrays

The spectra acquired with different phase-encoding arrays are shown in Fig. 7. Compared with spectra acquired with the 16×16×8 array shown in Fig. 7, those acquired with the 12×12×8 array had a lower SNR and great lipid contamination. The latter condition is a universal dilemma in MRSI data with small FOVs. Since the SNR is proportional to the square root of scan time, the theoretical value of the difference in SNRs for spectral 16×16×8 and 12×12×8 arrays is approximately 1.33. From the patients' data (156 voxels), the SNRs of the Cho, Cr and NAA in the 3 T spectra that were acquired with 16×16×8 phase-encoding steps were 1.19, 1.29 and 1.27 times, respectively, higher than the corresponding 12×12×8 data. The ratio from the patients was thus close to the theoretical value.

4. Discussion

Although PRESS H-1 MRSI is a powerful tool for providing metabolite profiles for patients with brain tumors, the spatial resolution obtained on 1.5-T scanners with a standard quadrature head coil is relatively coarse (1–2 cm) and the acquisition time is typically long (10–20 min). The availability of higher field strength MR scanners and multichannel radiofrequency coils offers the potential for

obtaining MRSI data with a higher SNR and better spectral resolution for such patients but also introduces complications in terms of the magnitude of the chemical shift artifact, increased susceptibility, differences in relaxation times and the need for more complex reconstruction algorithms. The objectives of our study were to determine how these factors affect the application of MRSI in patients with brain tumors and to establish a protocol that would provide robust and good quality data.

The first issue that we considered was the effect of chemical shift artifacts. Spectra simulated with ideal and empirical profiles showed the anticipated two-fold increase in effect with the field strength, but the artifact decreased rapidly with increasing overpress factors. Note that the magnitude of the effect depended on whether ideal or empirical profiles were used in the simulation. This was due to the larger transition bands of the empirical pulses resulting in imperfect edge excitation. Simulations representing a uniform phantom and normal brain with empirical profiles demonstrated that 40 mm VSS pulses and an overpress factor of 1.3 would be needed to eliminate the chemical shift artifact completely for selected volumes that were representative of those used in patient studies. Because it was felt that the magnitude of residual subcutaneous lipids would be unacceptable with an overpress factor of 1.3, the value used for empirical studies was 1.2.

The empirical data confirmed that the use of VSS pulses and increased overpress factors significantly reduced the chemical shift artifact in the eight-channel and the quadrature head coils. However, as predicted by the simulations, the spectra at 3 T were still not completely uniform. Their residual effects could be corrected by applying numerical factors determined from the simulations to the edge voxels to obtain accurate Cho/NAA ratios or by using selection pulses with higher bandwidths (e.g., spatial/spectral pulses) [26]. In this context, it should be noted that the default overpress factor in the product pulse sequences on most manufactured scanners is 1.0. If the radiologist is not familiar with this effect, then there is a danger of overcalling tumors on one side of the selected volume and undercalling them on the other. Clearly, it would be much safer to either apply appropriate overpress factors or use other means to correct for the chemical shift artifact. While the artifact is present at both field strengths, it is further accentuated at 3 T.

Another potential concern at a higher field strength has been the anticipated increase in linewidths due to larger susceptibility artifacts. In a previous article, the authors claimed that improvements in the SNR at 3 T were almost offset by the peak broadening [13]. In the current study, the estimated linewidths for Cho, Cr and NAA at 1.5 T were 0.071 ± 0.019, 0.067 ± 0.016 and 0.082 ± 0.022 ppm, respectively, at 1.5 T and were 0.051 ± 0.011, 0.048 ± 0.009 and 0.054 ± 0.010 ppm, respectively, at 3 T. Hence, the peak separation at 3 T was still better than that at 1.5 T for the healthy volunteers and patients. This implies that the higher-order shimming provided by the manufacturer worked well for the PRESS selected volume despite the presence of surgical cavities and other treatment effects.

The increased SNRs at 3 T that we observed were 1.67 for phantoms and 1.36 for healthy volunteers at 3 T versus 1.5 T with the quadrature head coil. The corresponding values for the eight-channel coils were 1.95 for phantoms, 1.54 for healthy volunteers and 1.50 for patients. We believe that the differences in the magnitude of the field strength effect between coils reflect that the 3 T quadrature coil was not optimized for data acquisition at this field strength and that the values from the eight-channel coil are more representative of the true benefits that can be obtained. Previous studies comparing 1.5 and 3 T with single-voxel and multivoxel proton MRS obtained similar increases in the SNR [14,15]. The differences in the magnitude of the effect between the phantom and human studies are due to known differences in the in vivo relaxation times at the two field strengths. The T_1 values of metabolites at 3 T are longer and the T_2 values are shorter than the data found at 1.5 T [16,17], which would result in a reduction in signal when using the same TR/TE. The change of differences in SNRs due to relaxation was computed by using T_1 and T_2 values of occipital gray matter reported in articles [16,17]. The 3 T to 1.5 T signal ratio of NAA would have increased by 10% in applying the T_1 correction and by a further 24% in applying the T_2 correction.

Of particular interest is that the SNR obtained at 3 T with the eight-channel coil was on average 2.33 times higher in healthy volunteers than for the current standard, which is using the quadrature head coil at 1.5 T. This means that there is considerable scope for improving the spatial resolution or shortening the acquisition time for patients with brain tumors using the new hardware. Other possibilities are to use the improved spectral resolution to obtain more reliable quantification and to apply improved detection of metabolites other than Cho, Cr and NAA [15]. The improved SNR for the phased-array coils [27] is a result of each coil element only detecting tissue noise from a limited tissue volume and the fact that the signals can be combined to provide an extended spatial coverage. In our study, we reconstructed spectra from the eight-channel coil using the empirical profiles derived from a calibration sequence that the manufacturer provides for parallel imaging. This proved to be robust but required independent phase and frequency correction for each channel before the signals were combined.

As a first step in examining the potential for shorter acquisition times with the 3 T and eight-channel coil, we compared spectra acquired from patients with two matrix sizes that had scan times of 9 and 17 min. Spectra acquired with the more limited phase-encoding array and shorter acquisition time were found to have a lower SNR, which was consistent with theoretical expectations. However, due to the smaller FOV, subcutaneous lipids were more likely to be folded in with the smaller matrix using the same nominal spatial resolution. More robust methods need to be developed to correct for lipids so as to benefit from the

shorter data acquisition time. One possibility is the use of parallel imaging reconstruction methods for lipid unfolding based on SENSE [28]. When combined with the use of 3 T MR scanners and multichannel radiofrequency coils, these methods will provide robust MRSI data from patients with brain tumors in a much shorter scan time.

5. Conclusion

We have demonstrated an increase in SNR at 3 T and with the eight-channel phased-array head coil in 3D H-1 MRSI data. The improved SNR obtained at 3 T with the eight-channel coil could be used to provide finer spatial resolution with the same acquisition time or to reduce the acquisition time to the more clinically relevant range of 5–9 min. The development of multichannel coils enhances the quality of spectra. The future application of larger coil arrays and even higher field strengths, such as 7 T, may further improve the SNR of such spectra.

Acknowledgment

This research was funded by a National Institutes of Health grant (P50 CA97257) and a University of California Discovery grant jointly with GE Healthcare (LSIT-10107).

References

[1] Fulham MJ, Bizzi A, Dietz MJ, Shih HH, Raman R, Sobering GS, et al. Mapping of brain tumor metabolites with proton MR spectroscopic imaging: clinical relevance. Radiology 1992;185(3):675–86.
[2] Preul MC, Caramanos Z, Collins DL, Villemure JG, Leblanc R, Olivier A, et al. Accurate, noninvasive diagnosis of human brain tumors by using proton magnetic resonance spectroscopy. Nat Med 1996;2(3):323–5.
[3] Nelson SJ, Huhn S, Vigneron DB, Day MR, Wald LL, Prados M, et al. Volume MRI and MRSI techniques for the quantitation of treatment response in brain tumors: presentation of a detailed case study. J Magn Reson Imaging 1997;7(6):1146–52.
[4] Preul MC, Caramanos Z, Leblanc R, Villemure JG, Arnold DL. Using pattern analysis of in vivo proton MRSI data to improve the diagnosis and surgical management of patients with brain tumors. NMR Biomed 1998;11(4–5):192–200.
[5] Nelson SJ. Multivoxel magnetic resonance spectroscopy of brain tumors. Mol Cancer Ther 2003;2(5):497–507.
[6] Pirzkall A, Li X, Oh J, Chang S, Berger MS, Larson DA, et al. 3D MRSI for resected high-grade gliomas before RT: tumor extent according to metabolic activity in relation to MRI. Int J Radiat Oncol Biol Phys 2004;59(1):126–37.
[7] McKnight TR, Noworolski SM, Vigneron DB, Nelson SJ. An automated technique for the quantitative assessment of 3D-MRSI data from patients with glioma. J Magn Reson Imaging 2001;13(2):167–77.
[8] Tran TK, Vigneron DB, Sailasuta N, Tropp J, Le Roux P, Kurhanewicz J, et al. Very selective suppression pulses for clinical MRSI studies of brain and prostate cancer. Magn Reson Med 2000; 43(1):23–33.
[9] Hattori N, Abe K, Sakoda S, Sawada T. Proton MR spectroscopic study at 3 Tesla on glutamate/glutamine in Alzheimer's disease. NeuroReport 2002;13(1):183–6.
[10] Gruber S, Mlynarik V, Moser E. High-resolution 3D proton spectroscopic imaging of the human brain at 3 T: SNR issues and application for anatomy-matched voxel sizes. Magn Reson Med 2003; 49(2):299–306.
[11] Jeun SS, Kim MC, Kim BS, Lee JM, Chung ST, Oh CH, et al. Assessment of malignancy in gliomas by 3T ^{1}H MR spectroscopy. Clin Imaging 2005;29(1):10–5.
[12] Wellard RM, Briellmann RS, Jennings C, Jackson GD. Physiologic variability of single-voxel proton MR spectroscopic measurements at 3T. AJNR Am J Neuroradiol 2005;26(3):585–90.
[13] Barker PB, Hearshen DO, Boska MD. Single-voxel proton MRS of the human brain at 1.5T and 3.0T. Magn Reson Med 2001;45(5): 765–9.
[14] Gonen O, Gruber S, Li BS, Mlynarik V, Moser E. Multivoxel 3D proton spectroscopy in the brain at 1.5 versus 3.0 T: signal-to-noise ratio and resolution comparison. AJNR Am J Neuroradiol 2001;22(9): 1727–31.
[15] Srinivasan R, Vigneron D, Sailasuta N, Hurd R, Nelson S. A comparative study of myo-inositol quantification using LC model at 1.5 T and 3.0 T with 3D ^{1}H proton spectroscopic imaging of the human brain. Magn Reson Imaging 2004;22(4):523–8.
[16] Mlynarik V, Gruber S, Moser E. Proton T (1) and T (2) relaxation times of human brain metabolites at 3 Tesla. NMR Biomed 2001; 14(5):325–31.
[17] Ethofer T, Mader I, Seeger U, Helms G, Erb M, Grodd W, et al. Comparison of longitudinal metabolite relaxation times in different regions of the human brain at 1.5 and 3 Tesla. Magn Reson Med 2003; 50(6):1296–301.
[18] Wald LL, Moyher SE, Day MR, Nelson SJ, Vigneron DB. Proton spectroscopic imaging of the human brain using phased array detectors. Magn Reson Med 1995;34(3):440–5.
[19] Nelson SJ, Vigneron DB, Star-Lack J, Kurhanewicz J. High spatial resolution and speed in MRSI. NMR Biomed 1997;10(8): 411–22.
[20] Wright SM, Wald LL. Theory and application of array coils in MR spectroscopy. NMR Biomed 1997;10(8):394–410.
[21] Natt O, Bezkorovaynyy V, Michaelis T, Frahm J. Use of phased array coils for a determination of absolute metabolite concentrations. Magn Reson Med 2005;53(1):3–8.
[22] Nelson SJ. Analysis of volume MRI and MR spectroscopic imaging data for the evaluation of patients with brain tumors. Magn Reson Med 2001;46(2):228–39.
[23] Li X, Vigneron DB, Cha S, Graves EE, Crawford F, Chang SM, et al. Relationship of MR-derived lactate, mobile lipids, and relative blood volume for gliomas in vivo. AJNR Am J Neuroradiol 2005;26(4): 760–9.
[24] Pruessmann KP, Weiger M, Scheidegger MB, Boesiger P. SENSE: sensitivity encoding for fast MRI. Magn Reson Med 1999;42(5): 952–62.
[25] Zhang Y, Brady M, Smith S. Segmentation of brain MR images through a hidden Markov random field model and the expectation-maximization algorithm. IEEE Trans Med Imaging 2001; 20(1):45–57.
[26] Star-Lack J, Vigneron DB, Pauly J, Kurhanewicz J, Nelson SJ. Improved solvent suppression and increased spatial excitation bandwidths for three-dimensional PRESS CSI using phase-compensating spectral/spatial spin-echo pulses. J Magn Reson Imaging 1997; 7(4):745–57.
[27] de Zwart JA, Ledden PJ, van Gelderen P, Bodurka J, Chu R, Duyn JH. Signal-to-noise ratio and parallel imaging performance of a 16-channel receive-only brain coil array at 3.0 Tesla. Magn Reson Med 2004;51(1):22–6.
[28] Ozturk E, Cha S, Chang SM, Berger MS, Nelson SJ. Lipid unaliasing for MR spectroscopic imaging of gliomas at 3T utilizing sensitivity encoding (SENSE). Proc 13th ISMRM; 2005.